ACS APPLIED MATERIALS & INTERFACES

Research Article

www.acsami.org

Influence of Dopamine Concentration and Surface Coverage of Au Shell on the Optical Properties of Au, Ag, and $Ag_{core}Au_{shell}$ Nanoparticles

Yanru Bu and Sangwha Lee*

Department of Chemical and Biochemical Engineering, Gachon University, Seongnam City, Gyeonggi-Do, Republic of Korea

Supporting Information

ABSTRACT: Gold (Au), silver (Ag), and $Ag_{core}Au_{shell}$ nanoparticles (NPs) were explored as optical sensing agents for the sensitive detection of dopamine (DA) neurotransmitters in surface-enhanced Raman scattering (SERS) measurements. In these colloidal systems, dopamine (DA) molecules played as a cross-linker between M NPs (Au or Ag NPs), allowing them to reside in the confined junctions (i.e., hot spots) between aggregated NPs. The progressive addition of DA molecules (from 1×10^{-6} to 1×10^{-3} M) consequently decreased a primary absorption peak attributed to the characteristic M NPs and generated a secondary absorption peak at longer wavelengths attributed to heavily aggregated M NPs formed by molecular bridging effects of DA molecules at high concentrations. The aggregation degree of M NPs was also dependent on the surface states of Au and Ag NPs, i.e., DA molecules with positive amine groups induced more aggregations of Au NPs in comparison to Ag NPs with less negative charges. As the final outcome, Au NPs demonstrated higher sensitivity in SERS detection of DA at low concentrations (1×10^{-7} to 1×10^{-5} M), whereas Ag NPs exhibited the stronger Raman signals of DA molecules at high concentrations (1×10^{-4} to 1×10^{-3} M). Besides, $Ag_{core}Au_{shell}$ NPs with the lowest surface coverage of Au shell exhibited more sensitive and stronger SERS activity for DA molecules than that of singular Au NPs, probably due to the combined contribution by Ag core with strong SERS intensity and Au shell with high SERS sensitivity.

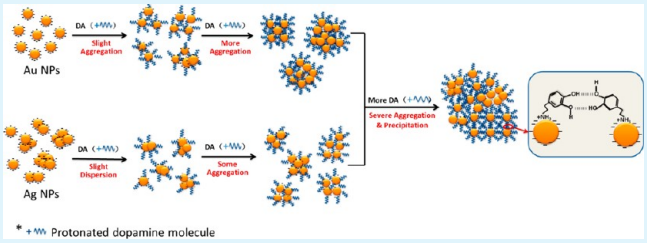

KEYWORDS: *Au, Ag, $Ag_{core}Au_{shell}$, dopamine, aggregation, plasmon absorption, SERS*

INTRODUCTION

Noble metallic nanoparticles (M NPs) are widely used as optical sensing agents for biorecognition because of their unusual optical and electronic properties. Especially, gold (Au) and silver (Ag) NPs have been of particular interest in spectroscopic analyses because of their intense visible-region absorption, which is largely attributed to the surface plasmon resonance (SPR).[1−3] Surface-enhanced Raman scattering (SERS) using M NPs can markedly magnify the Raman signals of the probe molecules by 1×10^6 to 1×10^{14} times, which makes sensitive detection and analysis of a single molecule possible.[4−10] In particular, bimetallic NPs with a core−shell structure often exhibit improved physical and chemical properties (such as unique optical, electronic, and catalytic properties) over their monometallic counterparts, due to a localized electric field enhancement in the core−shell structure.[11−14]

Specific ligands adsorbed on M NPs can influence the optical properties by affecting the SPR state of the metal surface and the aggregation state of colloidal NPs.[15,16] Thus, it is very important to understand the interaction behavior of specific ligands with M NPs to optimize the desired optical properties. The analyte used in this work was dopamine (DA), a neurotransmitter associated with proper functioning of several organs such as the heart, brain, and suprarenal glands. The quantitative detection of DA neurotransmitters is very important in the early detection of Parkinson disease. The plasmon absorbance of Au NPs allowed for the quantitative detection of DA neurotransmitter with a detection limit of 1×10^{-5} to 1×10^{-6} M.[17] A colorimetric determination of DA using Au NPs was used for highly selective method, in which DA with the help of Cu (II) induced the aggregation of Au NPs with a consequent color change.[18] Even though DA concentration can be quantified spectroscopically or visually, these methods are not sensitive enough to detect DA at low concentrations. Detecting DA with SERS has recently been recognized as a promising technique for direct neurotransmitter monitoring and research has focused on optimizing operating conditions and enhancing SERS substrates.[19−21] For instance, Ag colloids have been modified as aggregates by the addition of electrolytes[6] and/or complexed with iron(III) to obtain high SERS activity for DA molecules.[20]

M NPs prepared by the citrate reduction method are negatively charged due to citrate capping effect and stable with

Received: April 29, 2012
Accepted: July 25, 2012
Published: July 25, 2012

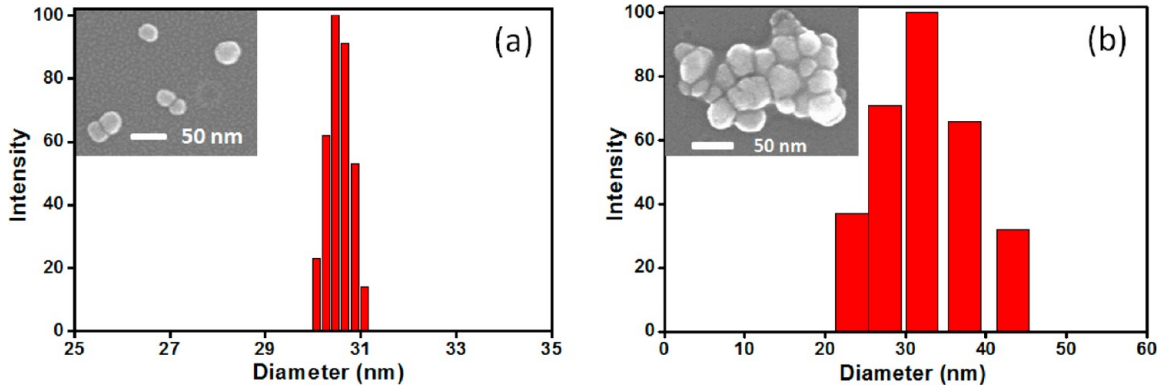

Figure 1. DLS size distribution of (a) Au NPs prepared by 0.5 mL of 1.0 wt % citrate and (b) Ag NPs prepared by 6 mL of 1.0 wt % citrate. Insets are the SEM images of the NPs.

the assistance of electrostatic repulsion.[22] When probe molecules with positive amine groups are added into colloidal M NPs, they adsorb onto the surface of the nanoparticles, which alters the surface charge state (or stability) of M NPs and affects the SPR state of M NPs.[23] In particular, bifunctional DA molecules can play as a cross-linker by forming hydrogen bonds between M NPs and thus inducing the aggregation of M NPs.[24] When the interparticle distance between M NPs is less than 5 nm, the electromagnetic field of neighboring M NPs would couple effectively and greatly enhance the Raman signal of the probe molecules adsorbed on M NPs.[23,25] Thus, aggregated form of M NPs would enhance the Raman intensity of probe molecules by providing additional hot spots in which the excitation energy is localized. However, severe aggregation of M NPs would weaken the Raman signal because of the decrease in hot spots caused by the precipitation of heavily aggregated M NPs.[22]

Some studies have examined the SERS activity of $Au_{core}Ag_{shell}$ core−shell NPs with DA molecules. In their SERS study of DA molecules adsorbed on $Au_{core}Ag_{shell}$ NPs, the vibration mode of the DA molecules assigned from the potential energy distributions and the pH-dependent Raman signal of the DA molecule in aqueous solution was recorded to elucidate the protonation effect and preferential existence of different forms of the DA molecule.[26] Practically, $Ag_{core}Au_{shell}$ NPs have more advantages than $Au_{core}Ag_{shell}$ NPs in SERS measurements; these include the following: (i) Ag is not as stable as Au, so that Ag is more apt to be oxidized and/or aggregated; (ii) Au is more sensitive than Ag to the specific ligands having −SH or $-NH_2$ functional groups. So, the Au shell can provide high sensitivity when detecting probe molecules with these functional groups;[23] and (iii) the surface morphology of Au shell is more controllable than that of Ag shell because of the relatively easy reduction of Au ions, which is meaningful for ensuring the stability and reliability in SERS measurement. Furthermore, the Ag core can provide extra enhancement of SERS activity to the Au shell.[8,27] Thus, it is plausible to assume that $Ag_{core}Au_{shell}$ NPs can bestow highly sensitive and reliable SERS activity for DA molecules.

In this work, we examined the effect of dopamine concentrations on optical properties of colloidal M NPs (Au and Ag NPs) prepared by citrate reduction method. The optical properties of colloidal M NPs were strongly dependent on the concentrations of DA molecules which consequently induced the aggregations of M NPs through their molecular bridging effects allowing DA molecules to reside in the confined junctions (i.e., hot spots) between aggregated NPs. The SERS signals of DA adsorbed on M NPs were also investigated as the function of DA concentrations. Interestingly, Au surface was more sensitive in the SERS detection of DA molecules at low concentrations (1×10^{-7} to 1×10^{-5} M), whereas Ag surface displayed the stronger SERS activity for DA molecules at high concentrations ($>10^{-4}$ M). This difference of SERS activity to DA molecules was interpreted as the different aggregation behaviors of Au and Ag NPs with DA concentrations, respectively. Furthermore, $Ag_{core}Au_{shell}$ NPs with controlled surface coverage of Au shell were prepared using the seed-growth method to optimize the SERS activity for DA molecules. Among them, $Ag_{core}Au_{shell}$ NPs with the lowest surface coverage of Au shell exhibited the highest SERS activity for DA molecules. This work can provide some insights in the SERS measurement using colloidal systems, highlighting the importance of molecular bridging effects (probe-induced aggregations) and surface coverage of Au shell in the sensitive detection of specific probe molecules with low detection limits.

EXPERIMENTAL SECTION

Materials. Chloroauric acid ($HAuCl_4$), silver nitrate ($AgNO_3$), sodium citrate ($Na_3C_6H_5O_7$), hydroxylamine hydrochloride ($NH_2OH{\cdot}HCl$), high-performance liquid chromatography (HPLC) grade water (H_2O), and dopamine hydrochloride ($C_8H_{11}NO_2{\cdot}HCl$) were purchase from Aldrich. All reagents are analytically pure.

Synthesis of Au NPs. Au NPs (20−80 nm) were prepared according to the citrate reduction method.[28,29] The particle size was controlled by adjusting the relative amounts of citrate ions to ionized gold complex in aqueous solution. Au NPs were obtained by the injection of suitable volume of 1.0 wt % sodium citrate (0.2−0.5 mL) into 50 mL of boiling water containing 0.5 mL of 1.0 wt % $HAuCl_4$. When the color changed from black (deep-blue) to red in 2 min, the reaction flask was immediately removed from the hot plate and transferred to a cold plate. Stirring was maintained until the solution was cooled down to room temperature.

Synthesis of Ag NPs. Ag NPs (20−50 nm) were prepared according to the modified citrate reduction method.[30] An aliquot volume of 2 mL, 4 mL, or 6 mL of 1.0 wt % sodium citrate was injected rapidly into 100 mL of a boiling solution containing 1.0 mL of 1.0 wt % $AgNO_3$ with vigorous stirring. The mixture was kept boiling for 10 min prior to cooling as described above.

Synthesis of $Ag_{core}Au_{shell}$ NPs. A two-step reduction in aqueous solution was used for the preparation of gold-coated silver NPs.[31] In brief, 12.5 mL of Ag precursor was diluted with 10 mL of HPLC grade water, and then x mL of 6.25×10^{-3} M $NH_2OH{\cdot}HCl$ and x mL of 4.65×10^{-4} M $HAuCl_4$ were added dropwise at an approximate rate of 2 mL/min by two separate pipets into the mixture with vigorous stirring. The stirring was continued for 45 min. The surface coverage

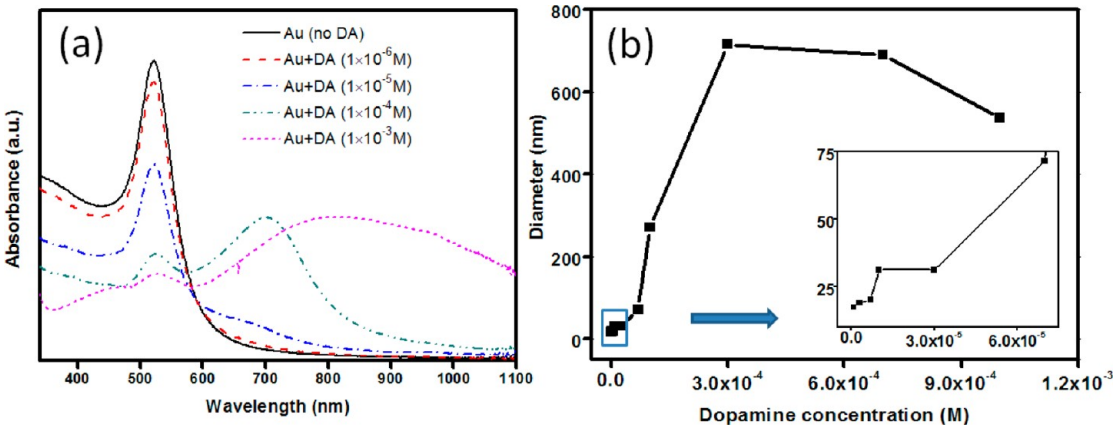

Figure 2. (a) UV−vis spectra of Au NPs (20 ± 5 nm) with different concentration of dopamine (DA) (1×10^{-6} to 1×10^{-3} M). (b) Size of Au NPs with different DA concentrations according to DLS measurements.

of Au shell could be changed by adjusting the loading volumes of $NH_2OH{\cdot}HCl$ and $HAuCl_4$ solution. In this work, three different $Ag_{core}Au_{shell}$ NPs were prepared by the injection of 2, 4, and 6 mL of 6.25×10^{-3} M $NH_2OH{\cdot}HCl$ and 4.65×10^{-4} M $HAuCl_4$ into reaction solution.

Characterization. The optical properties of Au, Ag, and $Ag_{core}Au_{shell}$ NPs were investigated with different concentrations of DA. A predetermined concentration of DA was injected into Au, Ag, and $Ag_{core}Au_{shell}$ NPs and stirred for 30 min. After then, an Agilent 8453 diode array spectrophotometer UV−vis spectrometer and Monora500i micro Raman spectrometer (ANDOR) were used to characterize the optical properties of these M NPs. The Raman spectrograph employed a 1200 g/mm grating and laser excitation at 632.8 nm, with accumulation times of 5 s. DLS (BI−HV; Brookhaven Instrument) and field emission (FE)-SEM (Hitachi) were also employed to investigate the size and morphology of as-prepared samples.

RESULTS AND DISCUSSION

Figure 1 shows the size distribution of Au NPs and Ag NPs prepared by different amounts of citrate ions, with SEM images provided in the accompanying inserts. The SEM and DLS analyses revealed that Au NPs exhibited the more uniform distribution of particle size as compared to Ag NPs. For the latter NPs, the increase of citrate ions relative to ionized silver complex did not produce a significant change of particle size, but rather induced the change of particle shape from smooth and spherical to a more edged and nonspherical morphology (data not shown). The reason may be that the two nearest carboxylate groups of citrate ions would selectively adhere to Ag (111) facets and grow along these facets.[32] On the other hand, the particle size of Au NPs was facilely controlled by varying the citrate amounts relative to ionized gold complex; i.e., the particle size was decreased with the increase of citrate amount.

Figure 2a shows the UV−vis spectra of Au NPs with different concentrations of DA. Au NPs approximately 20 nm in size produced a SPR absorption peak at around 520 nm. When the concentration of DA was increased, the peak at 520 nm was gradually decreased and slightly red-shifted, accompanyied with the appearance of a slight secondary peak at longer wavelength for a DA concentration of 10^{-5} M. Further increase of DA concentration intensified the secondary peak with a more distinct red-shift. Figure 2b shows the size of aggregated Au NPs (or Au clusters) with different concentrations of DA. For low DA concentrations (1×10^{-6} to 1×10^{-5} M), the size of Au clusters was slightly increased. Upon further increase of DA concentration, the size of Au clusters were gradually increased up approximately 70 nm, followed by the rapid increase of cluster size until a DA concentration of 3×10^{-4} M. When the concentration of DA was increased over 3×10^{-4} M, the size of Au clusters were gradually decreased, probably due to some precipitation of heavily aggregated Au NPs.

When the concentration of DA was very low in the colloid solution ($<10^{-5}$ M), DA was first adsorbed at a low density on the surface of Au NPs.[33] The Au NPs capped by citrate ions should be negatively charged, and DA with amino group is positively charged below pH9.[34] Thus, the amino group of DA can be easily adsorbed onto the surface of Au NPs via electrostatic interactions.[35]

According to the Mie theory, the SPR mainly depends on the free Elecron density of M NPs. When the chemical bond exists between adsorbed molecules and the M NPs, charge transfer would occur between them and change the free electron density of the M NPs. If the electron transfer from the M NPs to adsorbed molecule, the SPR would be red-shifted. Conversely, if the electron transfer from adsorbed molecule to M NPs, the free electron density would be increased and the SPR would be blue-shifted. The SPR absorption wavelength of NPs (λ_p), which is influenced by the free electron density, can be described by the equation

$$\lambda_p = 2\pi c/\omega_p \quad (1)$$

where c is the velocity of light in a vacuum and ω_p is the metal's bulk plasma frequency, given by

$$\omega_p = (N_e^2/m\varepsilon_0)^{1/2} \quad (2)$$

where N_e is the free electron density and m is the electron mass.[23]

When DA ligand adsorbed on the surface of Au NPs, the amino group of DA would attract the free electrons of Au NPs. As a result, the free electron density of M NPs, N_e, would decrease and consequently lead to the decrease of ω_p according to eq 2. Finally, the adsorption of DA on the M NPs induced the increase of λ_p according to eq 1, leading to the slight red-shift of SPR absorption peak, which was experimentally confirmed by the absorption peaks of Au NPs shown in Figure 2a.

When the concentration of DA was further increased to 1×10^{-4} M, a new absorption peak appeared at a longer

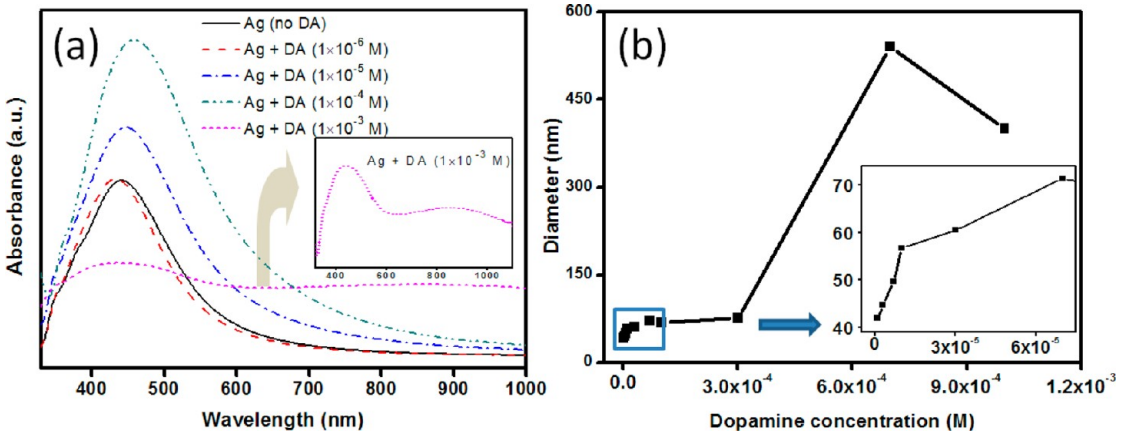

Figure 3. (a) UV−Vis spectra of Ag NPs (40 ± 10 nm, pH 6) with different concentrations of DA (1×10^{-6} to 1×10^{-3} M). (b) Diameter of Ag NPs with different concentrations of DA according to DLS measurements.

wavelength, indicating a change in the NP morphology from isolated domains to aggregated domains. According to Figure 2b, when the concentration of DA was higher than 1×10^{-4} M, the particle size of Au clusters was obviously increased. While at higher DA concentations (1×10^{-4} to 1×10^{-3} M), the extent of aggregation was increased significantly. As a result, the aggregated Au NPs generated a new absorption peak at longer wavelengths due to dipole−dipole coupling between the plasmons of neighboring Au NPs.[36,37]

The aggregation behavior of M NPs in the presence of DA molecules can be interpreted by the electric double layer (EDL) balance breaking and/or molecular bridging effects. The amine group binding to the surface of M NPs via electrostatic interactions would break the electronic balance of the NPs. Thus, the stability of the NPs would be decreased and the resulting NPs tend to aggregate due to the disturbance of electric double layer (EDL). However, if the concentration of DA is sufficiently high, the bridging effect becomes dominant. When the solution pH is less than ca. pH10, intermolecular hydrogen bonding interactions between neighboring −OH groups of DA adsorbed on M NPs would overcome the interparticle repulsive forces and finally lead to aggregation of M NPs.[18,24] That is, bifunctional DA molecules can play as a cross-linker through the hydrogen-bonding between the protruding hydroxyl groups of DA adsorbed on M NPs. Figure S1 (in the Supporting Information) showed the comparative difference, in that Au NPs without DA were discretely distributed on the copper grid, but Au NPs with 5×10^{-5} M of DA displayed some directional and/or tightly aggregated Au NPs on the copper grid, probably due to the interplaying cross-linking effects on the NPs by DA molecules.[40]

To examine the existence of molecular bridging effect in details, we prepared two different types of Au NPs with the same zeta potentials. One is the Au NPs with DA molecules (5×10^{-5} M), of which the zeta potential was −32.24 mV, and another is the dopamine-free Au NPs with the almost same zeta potential (−31.74 mV), adjusted by pH control. In reference, the zeta potential and particle size of original Au NPs were −39.75 mV and 27 nm, respectively. When compared to the original Au NPs, the absorption peak of dopamine-free Au NPs (−31.74 mV) was slightly red-shift and the particle size was increased by 19 nm, mainly due to the electronic disturbance by pH adjustment (see Figure S2 in the Supporting Information). On the other hand, the absorption peak of Au NPs with 5×10^{-5} M of DA was greatly red-shifted accompanying with the secondary peak at longer wavelength (ca. 650 nm). The particle size was fairly increased up to ca. 70 nm, indicating that DA played as a cross-linker to induce more aggregation of Au NPs. Even though the two Au NPs had the same zeta potentials, more serious aggregation was observed only to Au NPs with high concentration of DA due to their molecular bridging effects.

Figure 3a shows the UV−vis spectra of Ag NPs (ca. 40 nm) with different concentrations of DA. The Ag NPs displayed a strong SPR absorption peak around 430 nm. With low concentrations of DA, the peak position was slightly blue-shifted. When the concentration of DA was increased from 10^{-6} M to 10^{-4} M, the absorption peak position was gradually red-shifted, and the absorption intensity intensified. The excessive addition of DA concentration (approximately 1×10^{-3} M) significantly decreased the intensity of the primary peak with the simultaneous appearance of the secondary peak at longer wavelength, which was very similar to Au NPs. Figure 3b displays the size variation of aggregated Ag NPs (or Ag clusters) with different concentrations of DA. Even up to a high concentration of DA (3×10^{-4} M), the size of Ag clusters was slightly increased and was maintained at less than approximately 70 nm. For higher concentrations exceeding 3×10^{-4} M, the size of Ag clusters was significantly increased with rising concentrations of DA, followed by the rapid decrease of cluster size, probably because of the precipitation of heavily aggregated Ag NPs.

Because the surface charge of Ag NPs was less negative than that of Au NPs, their electrostatic repulsion was less able to overcome the attractive forces between M NPs, consequently leading to the formation of some clusters during NP synthesis.[22] In practice, the zeta potentials of Au NPs and Ag NPs were measured as −39.75 and −11.70 mV, respectively. The slight addition of DA molecules seemed to act as both a dispersive agent and a weak cross-linking agent, even up to interemdiate concentrations (1×10^{-6} to 1×10^{-4} M). That is, the size of Ag clusters was kept within approximately 70 nm, corresponding to small clusters comprising three or four Ag NPs (Figure 3b). In addition, the SPR absorption peak was more intensified with rising concentrations of DA. For the excessive addition of DA (>3×10^{-4} M), the molecular bridging effect became strong enough to induce the copious aggregation of Ag NPs and subsequent precipitation.

The proposed aggregation behavior of metallic NPs with DA concentration is summarized in Figure 4. Au NPs were stable

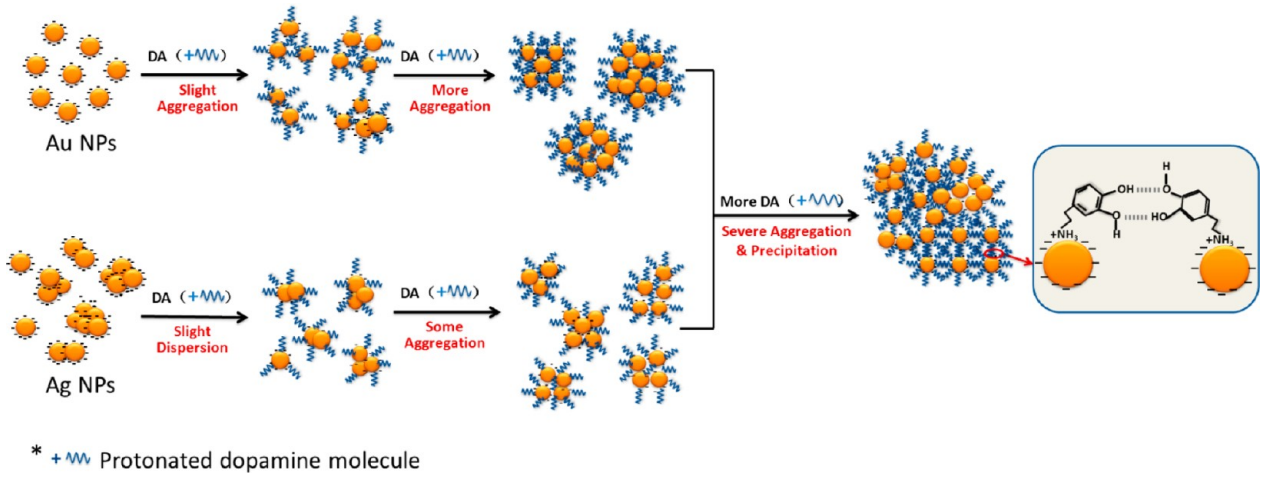

Figure 4. Behavior of metallic NPs with increasing DA concentrations.

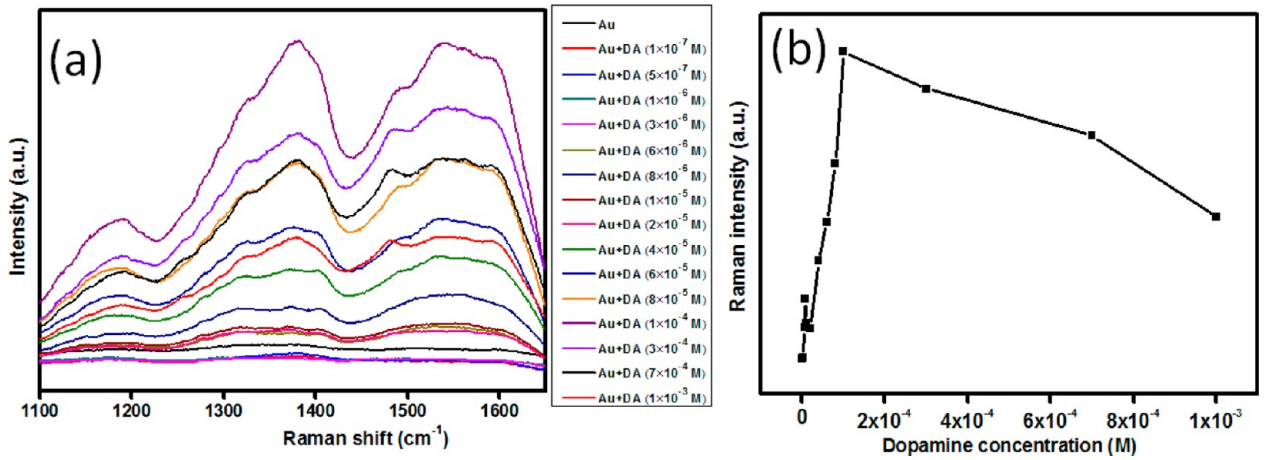

Figure 5. (a) Raman spectra of different concentrations of DA (1×10^{-7} to 1×10^{-3} M) adsorbed on Au NPs, (b) Raman intensity of DA adsorbed Au NPs at 1480 cm^{-1} with increasing concentrations of DA.

due to the citrate capping effect, which can induce electrostatic repulsions between M NPs. When DA with a protonated amine group was added, adsorption of DA initially occurred on the surface of Au NPs, subsequently inducing the aggregation of M NPs through hydrogen-bond-mediated cross-linking. With the increase of DA concetrations, the Au NPs would aggregate more and finally precipitate. On the other hand, Ag NPs only slightly aggregated due to reduced electrostatic repulsion caused by weakly bound citrate ions. The result was many aggregated clusters of Ag NPs. Thus, the progressive addition of DA first induced the dispersion effect on clustered M NPs and disintegrated into very many small clusters comprising three or four Ag NPs, which resulted in intensified absorption bands of Ag NPs. When compared wth Au NPs, the molecular bridging effect of DA was not strong enough to induce large cluster formation of Ag NPs. However, the excessive addition of DA induced pronounced aggregation of Ag NPs, leading to the precipitation of heavily aggregated Ag NPs.

In summary, DA concentration can strongly influence aggregation of M NPs and the resultant optical properties. Thus, it is plausible to suggest that DA concentration can strongly affect the SERS signal on M NPs with different extents of aggregation.

Figure 5a shows the Raman spectra of DA molecules absorbed on Au NPs with different concentrations (1×10^{-7} to 1×10^{-3} M). The observed peak of DA might be unclear probably due to the florescence interfering and/or the heat effect induced by high energy exciting laser of 632.8 nm. The relatively obvious peak at around 1480 cm^{-1} was assigned to the phenolic CH_2 stretching mode of DA,[26] which appeared as a more distinct shape with increased DA concentration. Thus, the peak intensity at 1480 cm^{-1} was plotted as the function of DA concentration to compare the SERS sensitivity of DA with different concentrations. As shown in Figure 5b, the Raman intensity of DA adsorbed on Au NPs was distinctly increased at low concentrations and then gradually decreased at high concentrations ($>1 \times 10^{-4}$ M), indicating that the aggregation state of M NPs was an important factor in the SERS measurment of DA. When the M NPs were slightly aggregated by the molecular bridging effect of DA at low concentrations (1×10^{-7} to 1×10^{-4} M), they might offer more hot spots for SERS enhancement, corresponding to the particle size ranges from 20 to ca. 70 nm. However, when the DA concentration was higher than 1×10^{-4} M, the molecular bridging effect was strong enough to induce the copious aggregation of Au NPs, resulting in the decrease of the SERS intensity of DA. Only in an appropriate DA concentration range, where slight aggregation of M NPs occurred, would the Raman signal of DA exhibit strong SERS intensity. That is, the coupled electromagnetic field would markedly enhance the SERS signal

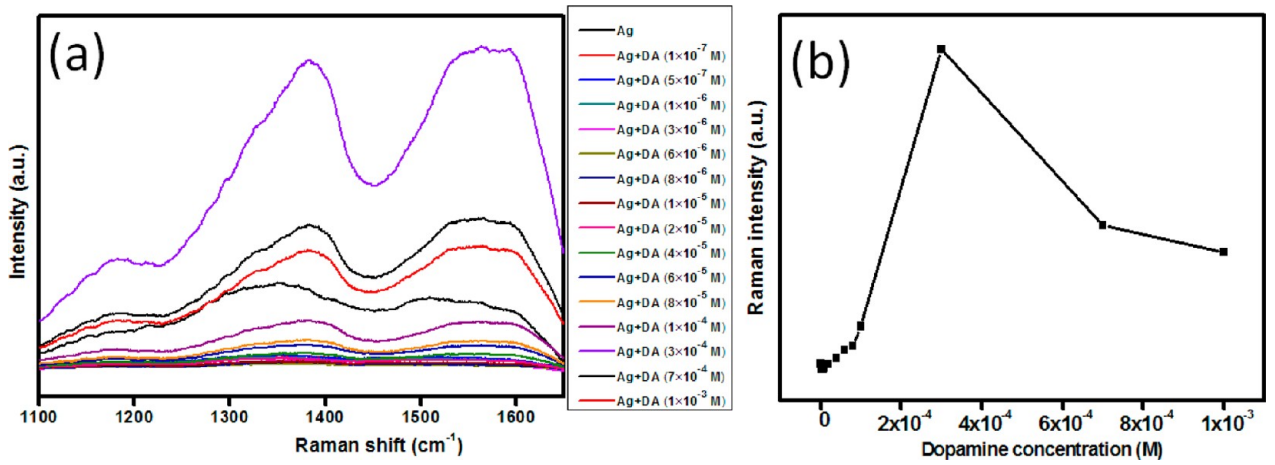

Figure 6. (a) Raman spectra of different concentrations of DA (1×10^{-7} to 1×10^{-3} M) adsorbed on Ag NPs. (b) Raman intensity of DA adsorbed on Ag NPs at 1590 cm^{-1} with increasing DA concentration.

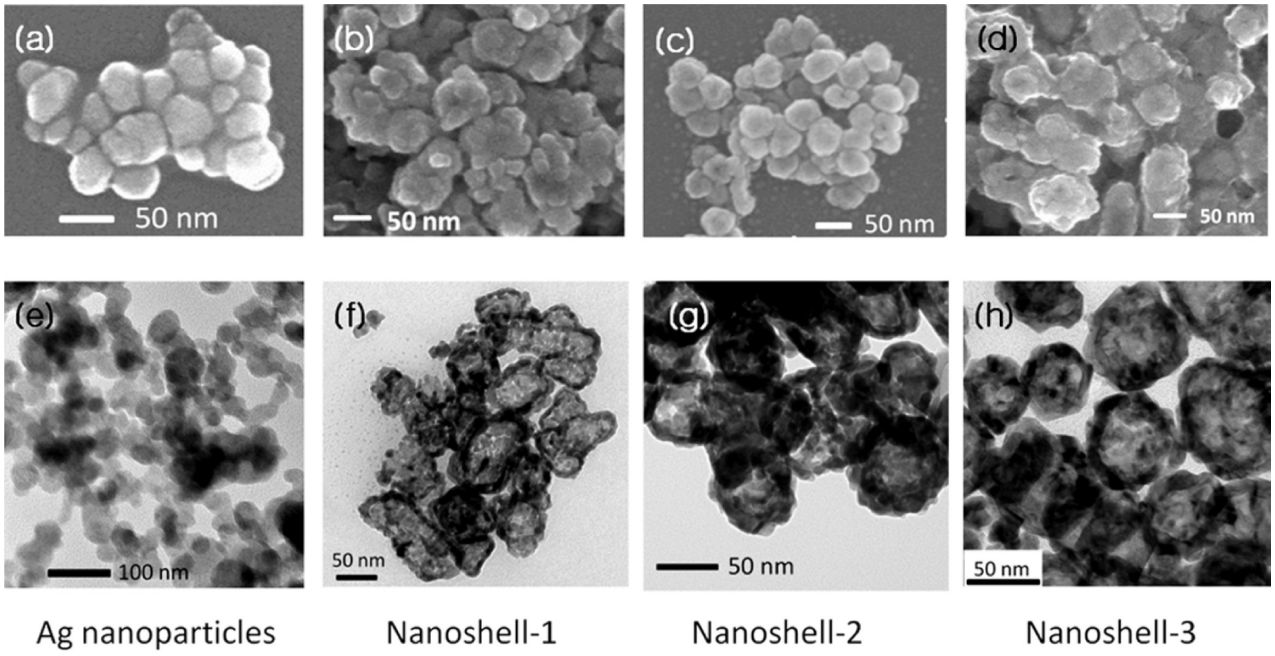

Figure 7. SEM and TEM images of Ag NPs and three kinds of $Ag_{core}Au_{shell}$ NPs: (a, e) SEM and TEM images of Ag NPs, (b, f) SEM and TEM images of $Ag_{core}Au_{shell}$ NPs prepared by 2 mL of $HAuCl_4$ (4.65×10^{-4} M) and 2 mL of $NH_2OH{\cdot}HCl$ (6.25×10^{-3} M), (c, g) SEM and TEM images of $Ag_{core}Au_{shell}$ NPs prepared by 4 mL of $HAuCl_4$ (4.65×10^{-4} M) and 4 mL of $NH_2OH{\cdot}HCl$ (6.25×10^{-3} M), (d, h) SEM and TEM images of $Ag_{core}Au_{shell}$ NPs prepared by 6 mL of $HAuCl_4$ (4.65×10^{-4} M) and 6 mL of $NH_2OH{\cdot}HCl$ (6.25×10^{-3} M).

when the interparticle distance was less than the critical distance of 5 nm.

Figure 6a shows the Raman spectra of different concentrations of DA (from 1×10^{-7} M to 1×10^{-3} M) absorbed on Ag NPs. Even though the characteristic peak of DA on Ag NPs was unclear, the relatively obvious peak at around 1590 cm^{-1} was assigned to ν_{8a} vibration modes of DA.[38] Figure 6b shows the variation of Raman intensity of DA adsorbed on Ag NPs at 1590 cm^{-1} with rising concentrations of DA. The Raman intensity of DA was slowly increased in the concentration ranges up to 1×10^{-4} M (Figure 6b). Further increase of DA concentration induced the significant increase of Raman intensity followed by the rapid decrease over 3×10^{-4} M corresponding to the critical concentration for inducing copious aggregation of Ag NPs, as previously shown in Figure 5b.

When comparing Figures 5 and 6, Au NPs exhibited more highly sensitive detection of DA by SERS at low DA concentrations (1×10^{-7} to 1×10^{-4} M) as compared to Ag NPs. The secondary peak contributing to aggregated Au NPs appeared when DA concentration was 1×10^{-5} M, whereas the secondary peak of Ag NPs appeared when DA concentration was as high as about 10^{-3} M (Figure 2a). In other words, Au NPs exhibited higher affinity to positively charged DA as compared to Ag NPs. Even though Ag is known to have stronger (about 4-fold) SERS activity than that of Au, Au NPs exhibited more sensitive detection to DA molecules in low concentration ranges because the slight addition of DA induce small clusters of Au NPs with more hot spots, as determined by SERS measurments.

The Raman spectra of DA adsorbed on Au NPs was also examined in the presence of multifolds concentration of

ascorbic acid. According to the SERS measurements, the ascorbic acid does not affect the Raman spectra of DA molecules. In practice, ascorbic acid has no affinity to Au NPs so that it is very difficult for ascorbic acid to adsorb on the surfaces of Au NPs. Since the enhanced Raman signal is only observed for probe molecules adsorbed on the metallic surface, we conclude that nonadsorbing ascorbic acid cannot influence on the SERS signal of DA molecules in our colloidal system.

To improve the stability and sensitivity of M NPs as a SERS substrate for DA detection, we prepared $Ag_{core}Au_{shell}$ NPs with the view of "borrowing the high SERS intenstiy from Ag core and retaining the stability and sensitivity of Au shell".[7,23] With the aid of the long-range effect of electromagnetic enhancement fields created by Ag core and high stability and sensitivity attributed to Au shell, the $Ag_{core}Au_{shell}$ NPs were expected to confer high SERS activity to DA molecules. To prepare different Au shell thickness, small Ag NPs (approximately 25 nm) were prepared and subsequently used as Ag cores for Au shell formation. Figure 7 shows the SEM and TEM images of Ag NPs and $Ag_{core}Au_{shell}$ NPs prepared by adding 2, 4, and 6 mL of 4.65×10^{-4} M $HAuCl_4$ and 6.25×10^{-3} M $NH_2OH{\cdot}HCl$, respectively (hereafter referred to as nanoshell-1, nanoshell-2, and nanoshell-3, respectively). SEM revealed that $Ag_{core}Au_{shell}$ NPs exhibited more rough surface morphology than that of Ag NPs (Figure 7a). According to the TEM image of nanoshell-1 (Figure 7f), small size Au NPs were discontinuously covered on the surface of Ag core and some spots of Ag core surface were naked. In the TEM image of nanoshell-2 (Figure 7g), some of the Ag cores were wholly covered by Au shell, whereas some Ag cores were still half covered. In particular, some pinholes were observed in the SEM image of nanoshell-2. In the SEM image of nanoshell-3 (Figure 7d); however, all the Ag cores were wholly covered by Au shell. TEM image of the $Ag_{core}Au_{shell}$ NPs (Figure 7h) clearly demonstrated the core–shell nanostructure of $Ag_{core}Au_{shell}$ NPs.

According to the SEM and TEM images, our synthetic route seems to provide nanoparticles with a thin Au coating on a partially hollow Ag core due to gavanic replacement reaction. However, the nanoshell preapred by this method did not provide the strong red-shift of extinction maxima when caompared with hollow Au–Ag nanoshells reported by Lee and co-workers.[41] The reason may be that the reducing agent used in this work is strong enough to reduce gold acid immediately to minimize the generation of hollow interiors in the core–shell nanostructure.[31]

Figure 8 shows the UV–vis spectra of $Ag_{core}Au_{shell}$ NPs with different surface coverage of the Au shell. Nanoshell-1 (Ag core partially covered by the Au shell) had an absorption peak mainly attributed to the SPR of Ag NPs with a slight red-shift. Nanoshell-2, in which coverage of the Au shell was increased, had two distinct absorption peaks. The intensity of the first absorption peak was decreased and another absorption peak at longer wavelength (approximately 520 nm) appeared, which is the characteristic plasmon-derived absorption peak of Au NPs. Nanoshell-3 (full coverage of Au shell over the Ag core) exhibited a strong absorption peak at around 580 nm due to the complete formation of a core–shell nanostructue. This chemical strategy can be facilely used to design the optically tunable M NPs, of which the SPR absorption peak can be located in any position of visible-infrared wavelengh regions.

Figure 9 shows the Raman spectra of DA adsorbed on $Ag_{core}Au_{shell}$ NPs with different surface coverages of the Au shell. Nanoshell-1, which is only half covered by Au shell,

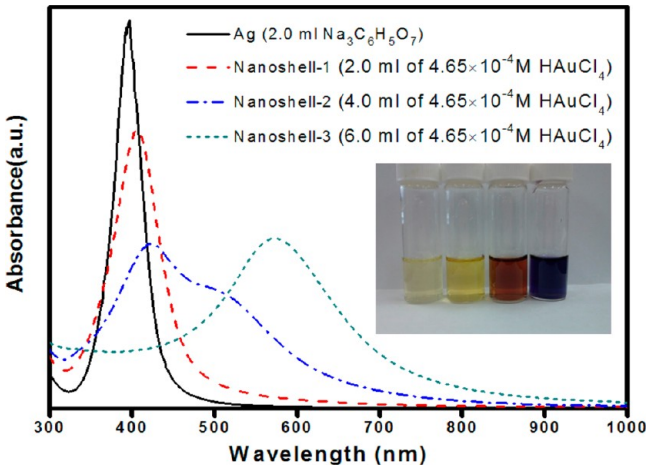

Figure 8. UV–visis spectra of Ag NPs (25 ± 5 nm) and $Ag_{core}Au_{shell}$ NPs prepared by different concentrations of Au precursor. Inset is the photograph of formed colloids.

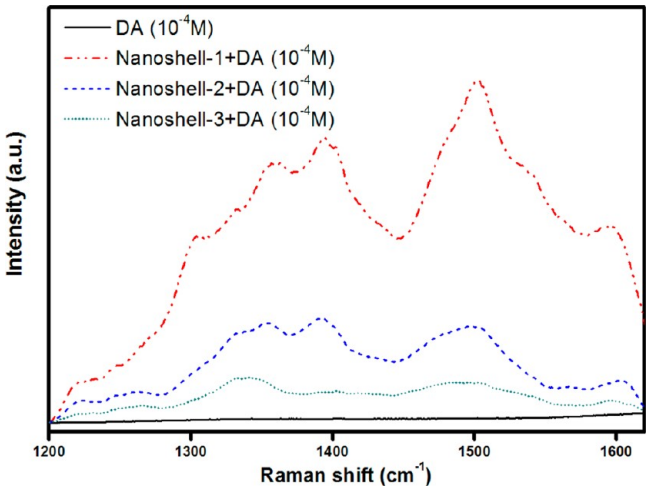

Figure 9. Raman spectra of DA (1×10^{-4} M) adsorbed on $Ag_{core}Au_{shell}$ NPs with different surface coverage of the Au shell.

clearly exhibited the strongest SERS signal among three types of nanoshells. The distinct SERS signal observed in nanoshell-1 could be mainly attributed to the punctiform naked Ag core with strong SERS activity. With the increase of Au shell coverage (nanoshell-1 < nanoshell-2 < nanoshell-3), the Raman signal was distinctly decreased because of the diminishment of effecive electromagnetic coupling between DA and higher-SRES-active Ag core.[39] Nanoshell-3 was wholly covered by Au shell with some thickness, but the Ag core can still enhance the Raman signal of adsorbed DA via its long-range electromagnetic field. When the thickness of Au shell was over a critical value, the SERS activity of nanoshells was fairly decreased because of the depletion of effecive electromagnetic coupling between DA and Ag core. However, all the $Ag_{core}Au_{shell}$ NPs exhibited higher enhancement factors in the SERS measurement when compared to the standard DA (1×10^{-4} M), indicating that SERS detection of DA using $Ag_{core}Au_{shell}$ is feasible.

Figure 10 shows the SERS spectra of DA (1×10^{-4} M) adsorbed on Au, Ag, and $Ag_{core}Au_{shell}$ NPs. Even though the different metallic NPs exhibited different enhancement factors for DA detection by SERS, all M NPs exhibited much higher

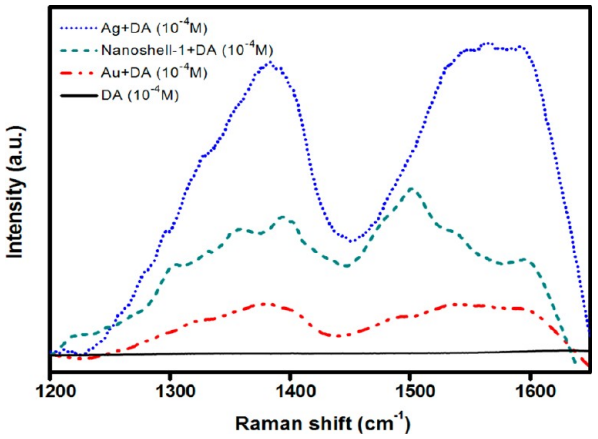

Figure 10. Raman spectra of DA (1×10^{-4} M) adsorbed on Au, Ag and $Ag_{core}Au_{shell}$ NPs prepared by 2 mL of $HAuCl_4$ (4.65×10^{-4} M) and 2 mL of $NH_2OH{\cdot}HCl$ (6.25×10^{-3} M).

Raman intensity than the standard DA itself. Even though Ag NPs showed the highest SERS intensity, Au NPs with the lowest SERS intensity exhibited the distinct Raman signal of DA molecules. On the other hand, $Ag_{core}Au_{shell}$ NPs (nanoshell-1) exhibited the higher SERS activity and more distinct SERS spectra of DA signature as compared to those of Au NPs. Since $Ag_{core}Au_{shell}$ NPs possess both high SERS activity of Ag core and high DA sensitivity of Au shell, the nanoshell structure is expected to display a high sensitivity to DA molecules in low concentration ranges ($<10^{-4}$ M), but also to demonstrate a high SERS intensity at high concentration ranges. Conclusively, $Ag_{core}Au_{shell}$ NPs with optimal Au shell thickness can be promising SERS substrates in the sensitive detection and analysis of DA neurotransmitters.

CONCLUSIONS

We have investigated the influence of dopamine concentration and surface coverage of Au shell on the optical characteristics of Au, Ag and $Ag_{core}Au_{shell}$ nanoparticles (NPs) as SERS-active substrates. With the increase of DA concentrations, the primary absorption peak of M NPs (Au and Ag NPs) was slightly red-shifted due to the change of SPR states of M NPs adsorbed with amino groups in DA. The further increase of DA concentrations generated a secondary absorption peak at longer wavelengths attributed to heavily aggregated M NPs formed by molecular bridging effects of DA molecules. What's more, the Raman intensity of DA adsorbed on M NPs was significantly affected by the DA concentrations (approximately proportional to molecular bridging effects of DA molecules) and surface states of M NPs. Interestingly, Au NPs demonstrated higher sensitivity in the SERS detection of DA molecules at low concentrations (1×10^{-7} M to 1×10^{-5} M), while Ag NPs displayed stronger Raman intensity at high concentrations ($>1 \times 10^{-4}$ M). Besides, $Ag_{core}Au_{shell}$ NPs with different surface coverage of Au shell showed the different degree of Raman enhancements to DA molecules. Among them, $Ag_{core}Au_{shell}$ NPs with the lowest coverage of Au shell exhibited more sensitive and stronger SERS activity for DA molecules than that of singular Au NPs, suggesting $Ag_{core}Au_{shell}$ NPs as a promising SERS substrate in the sensitive detection of DA neurotransmitters. These results can provide some insights in the SERS measurement using colloidal systems, highlighting the importance of molecular bridging effects and surface coverage of Au shell in the sensitive detection of dopamine molecules.

ASSOCIATED CONTENT

Supporting Information

TEM images of dopamine-free Au nanoparticles and Au nanoparticles with dopamine (1×10^{-4} M). UV–vis spectra of Au nanoparticles and corresponding DLS size distribution. This information is available free of charge via the Internet at http://pubs.acs.org/.

AUTHOR INFORMATION

Corresponding Author

*E-mail: Lswha@gachon.ac.kr.

Notes

The authors declare no competing financial interest.

ACKNOWLEDGMENTS

This work was supported by the National Research Foundation of Korea (NRF) grant funded by the Korea government (MEST) (20090093908) and by the National Research Foundation of Korea Grant funded by the Korean Government (MEST) (NRF-2010-C1AAA001-2010-0028958).

REFERENCES

(1) Kelly, K. L.; Coronado, E.; Zhao, L. L.; Schatz, G. C. *J. Phys. Chem. B* **2003**, *107*, 668–677.
(2) Daniel, M.; Astruc, D. *Chem. Rev.* **2004**, *104*, 293–346.
(3) Huang, X.; Jain, P. K.; El-Sayed, I. H.; El-Sayed, M. A. *Nanomedicine* **2007**, *2*, 681–693.
(4) Esenturk, E. N.; Walker, A. R. H. *J. Raman Spectrosc.* **2008**, *40*, 86–91.
(5) Hossain, M. K.; Kitahama, Y.; Huang, G. G.; Han, X.; Ozaki, Y. *Anal. Bioanal. Chem.* **2009**, *394*, 1747–1760.
(6) Kneipp, K.; Wang, Y.; Dasari, R. R.; Feld, M. S.; Gilbert, B. D.; Janni, J.; Steinfeld, J. I. *Spectrochim. Acta* **1995**, *51A*, 481.
(7) Cui, Y.; Ren, B.; Yao, J. L.; Gu, R. A.; Tian, Z. Q. *J. Phys. Chem. B* **2006**, *110*, 4002.
(8) Kneipp, K.; Kneipp, H.; Itzkan, I.; Dasari, R. R.; Feld, M. S. *Chem. Rev.* **1999**, *99*, 2957.
(9) Kumar, G. V. P.; Shruthi, S.; Vibha, B.; Reddy, B. A. A.; Kundu, T. K.; Narayana, C. *J. Phys. Chem. C* **2007**, *111*, 4388.
(10) Luo, J.; Zeng, G. M.; Tang, L.; Yin, J.; Li, Y. P. *Chin. J. Anal. Chem.* **2009**, *37*, 1847.
(11) Pande, S.; Ghosh, S. K.; Praharaj, S.; Panigrahi, S.; Basu, S.; Jana, S.; Pal, A.; Tsukuda, T.; Pal, T. *J. Phys. Chem. C* **2007**, *111*, 10806.
(12) Rivas, L.; Sanches-Cortes, S.; Garcia-Rameo, J. V.; Morcillo, G. *Langmuir* **2000**, *16*, 9722–9728.
(13) Yang, Y.; Shi, J.; Kawamura, G.; Nogami, M. *Scr. Mater.* **2008**, *58*, 862–865.
(14) Zaera, F. *J. Phys. Chem. B* **2002**, *106*, 4043.
(15) Gao, L. Z.; Zhang, X. T. *Acta Phys.Chim.Sin.* **2004**, *20*, 647.
(16) Ghosh, S. K.; Nath, S.; Kundu, S.; Esumi, K.; Pal, T. *J. Phys. Chem. B* **2004**, *108*, 13963.
(17) Baron, R.; Zayats, M.; Willner, I. *Anal. Chem.* **2005**, *77*, 1566.
(18) Zhang, Y. F.; Li, B. X.; Chen, X. L. *Microchim Acta.* **2010**, *168*, 107.
(19) An, J.; El-Said, W. A.; Yea, C.; Kim, T.; Choi, J. *J. Nanosci. Nanotechnol.* **2011**, *11*, 4424–4429.
(20) Kowalchyk, W. K.; Davis, K. L.; Morris, M. D. *Spectrochim. Acta* **1995**, *51A*, 145–151.
(21) Volkan, M.; Stokes, D. L.; Vo-Dinh, T. *Appl. Spectrosc.* **2000**, *54*, 1842–1848.
(22) Puebla, R. A.; Arceo, E.; Goulet, P. G.; Garrido, J.; Aroca, R. F. *J. Phys. Chem. B* **2005**, *109*, 3787.
(23) Ghosh, S. K.; Pal, T. *Chem. Rev.* **2007**, *107*, 4797.

(24) Mandal, S.; Gole, A.; Lala, N.; Gonnade, R.; Ganvir, V.; Sastry, M. *Langmuir* **2001**, *17*, 6262.
(25) Li, J. F.; Fang, P. P.; Sheng, J. J.; Bao, F.; Wu, D. Y.; Ren, B.; Tian, Z. Q. *J Light Scattering* **2007**, *19*, 358.
(26) Pande, S.; Jana, S.; Sinha, A. K.; Sarkar, S.; Basu, M.; Pradhan, M.; Pal, A.; Chowdhury, J.; Pal, T. *J. Phys. Chem. C* **2009**, *113*, 6989.
(27) Wei, S.; Wang, Q.; Zhu, J.; Sun, L.; Lin, H. F.; Guo, Z. H. *Nanoscale* **2011**, *3*, 4474.
(28) Enustun, B. V.; Turkevich, J. *J. Am. Chem. Soc.* **1963**, *85*, 3317.
(29) Frens, G. *Nat. Phys. Sci.* **1973**, *241*, 20.
(30) Lee, P. C.; Meisel, D. J. *Phys. Chem.* **1982**, *86*, 3391.
(31) Srnova-Sloufova, I.; Lednicky, F.; Gemperle, A.; Gemperlova, J. *Langmuir* **2000**, *16*, 9928.
(32) Zhang, Q.; Li, N.; Goebl, J.; Lu, Z. D.; Yin, Y. D. *J. Am. Chem. Soc.* **2011**, *133*, 18931.
(33) Basu, S.; Pande, S.; Jana, S.; Bolisetty, S.; Pal, T. *Langmuir* **2008**, *24*, 5562.
(34) Avendano, S. C.; Angeles, G. A. *J. Phys. Chem. B* **2007**, *111*, 1640.
(35) Raphael, L.; Nguyen, T. K. T.; Doty, R. C.; Hussain, I.; Nichols, R. J.; Schiffrin, D. J.; Brust, M.; Fernig, D. G. *J. Am. Chem. Soc.* **2004**, *126*, 10076.
(36) Kreibig, U.; Genzel, L. *Surf. Sci.* **1985**, *156*, 678.
(37) Storhoff, J. J.; Lazarides, A. A.; Mucic, R. C.; Mirkin, C. A.; Letsinger, R. L.; Schatz, G. C. *J. Am. Chem. Soc.* **2000**, *122*, 4640.
(38) Youn, M. Y.; Kim, Y. S.; Lee, N. S. *Bull. Korean Chem. Soc.* **1997**, *18*, 1314.
(39) Freeman, G. R.; Hommer, M. B.; Grabar, K. C.; Jackson, M. A.; Natan, M. J. *The J. Phys. Chem.* **1996**, *100*, 718.
(40) Li, W. C.; Lee, S. W. *Curr. Appl. Phys.* **2012**, *12*, 1361.
(41) Vongsavat, V.; Vittur, B. M.; Bryan, W. W.; Kim, J. H.; Lee, T. R. *ACS Appl. Mater. Interfaces* **2011**, *3*, 3616.